



Pergamon

SCIENCE @ DIRECT®

Bioorganic & Medicinal Chemistry Letters 13 (2003) 2473–2479

BIOORGANIC &  
MEDICINAL  
CHEMISTRY  
LETTERS

# Comparative Molecular Field Analysis (CoMFA) of Phthalazine Derivatives as Phosphodiesterase IV Inhibitors

Asit K. Chakraborti,\* B. Gopalakrishnan, M. Elizabeth Sobhia and Alpeshkumar Malde

Department of Medicinal Chemistry, National Institute of Pharmaceutical Education and Research (NIPER), Sector-67,  
S.A.S. Nagar 160 062, Punjab, India

Received 25 February 2003; revised 9 May 2003; accepted 9 May 2003

**Abstract**—A comparative molecular field analysis (CoMFA) of phthalazine class of phosphodiesterase IV (PDE IV) inhibitors has been performed to correlate their chemical structures with their observed biological activity. A statistically valid model with good correlative and predictive power is reported. The leave one out cross-validation study gave cross-validation  $r^2_{cv}$  of value 0.507 at six optimum components and conventional  $r^2$  of value 0.98. The predictive ability of the model was tested by predicting the seven molecules belonging to the test set giving predictive correlation coefficient of 0.59. This model is potentially helpful in the design of novel and more potent PDE IV inhibitors.

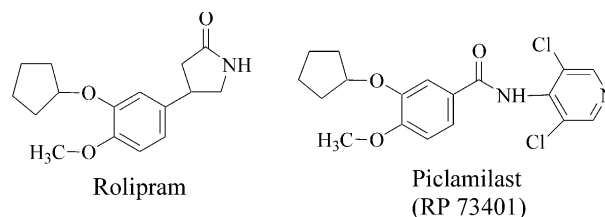
© 2003 Elsevier Ltd. All rights reserved.

## Introduction

Interest in the potential utility of isoenzyme selective phosphodiesterase (PDE) inhibitors has increased in recent years.<sup>1</sup> At least 11 families of PDE based upon a variety of criteria including substrate specificity, inhibition potency, enzyme kinetics, amino acid sequence, cellular and tissue distribution are known to exist.<sup>2</sup> Many pharmaceutical companies are attempting to discover the magic bullet for diseases like asthma and chronic obstructive pulmonary disease (COPD).<sup>3</sup> In this context, PDE type IV has been selectively targeted using chemical inhibitors on the basis of the clinical efficacy of the archetypal non-selective PDE inhibitor, theophylline, which has been used in the treatment of asthma and COPD.<sup>4</sup> PDE IV is a cyclic adenosine mono-phosphate (cAMP) specific enzyme showing very low affinity for cGMP. Four PDE IV subtypes have been cloned and expressed, with additional complexity arising as a consequence of m-RNA splicing resulting in isoforms with alterations in amino acid sequences within the N terminal region.<sup>5</sup> Analysis of amino acid sequence of PDE IV reveals a catalytic domain and two upstream conserved regions (UCRs) that are unique to this family of PDE.<sup>6</sup> The archetypal inhibitor rolipram<sup>7</sup> (Scheme 1)

has been the starting point for the majority of the medicinal chemistry efforts.<sup>8</sup> The research in this area dealing with the replacement of pyrrolidinone of rolipram with other functionalities led to discovery of piclamilast (RP-73401).<sup>9</sup> However, piclamilast was discontinued at phase two clinical trials due to undesirable side effects and poor pharmacokinetics.<sup>10</sup> The design of rigid analogues of piclamilast led to a series of phthalazine class of PDE IV inhibitors.<sup>11</sup>

Herein, we report the three-dimensional quantitative structure–activity relationship (3D-QSAR), using comparative molecular field analysis (CoMFA),<sup>12</sup> of a series of phthalazine class of PDE IV inhibitors. CoMFA, known for the renowned robustness of the model it produces,<sup>13,14</sup> has been used regularly to produce the 3D models to indicate the regions that affect the biological activity with a change in the chemical substitution. CoMFA models can describe the relative change in



Scheme 1.

\*Corresponding author. Tel.: +91-172-214682; fax: +91-172-214692;  
e-mail: akchakraborti@niper.ac.in

magnitude of the steric and electrostatic fields as a function of the sampled compounds chosen from dataset. The aim is to analyze structural requirements of this class of PDE IV inhibitors in terms of electrostatic and steric fields to understand structural basis for their affinity to the catalytic center of the enzyme and to design more potent inhibitors.

### Computational Details

#### Dataset for analysis

Reported in vitro data on two series of phthalazines<sup>11a–c</sup> and one series of dihydrophthalazines<sup>11d</sup> were used in the study (Table 1). The IC<sub>50</sub> values of 34 molecules were segregated into groups of 27 and 7 as training set and test set respectively. The IC<sub>50</sub> values were converted into pIC<sub>50</sub> according to the formula,

$$\text{pIC}_{50} = -\log_{10}\text{IC}_{50}$$

#### Computer modelling and structure alignment

The CoMFA<sup>12</sup> studies were performed using the software Sybyl 6.6<sup>15</sup> installed on a Silicon Graphics Power ONYX *extreme* workstation IRIX 6.5. Since the crystal structure of the PDE IV–inhibitor complex is not available, the least energy conformer was used as the bioactive conformation. The most active analogue amongst phthalazines, **23**, was subjected to conformational search using systematic search method in the Sybyl. The minimum energy conformer was taken and subjected to further minimization. The global minimum conformer thus obtained was taken as the template and rest of the structures were built from it. Initially, a constrained minimization for 100 cycles was performed to prevent the conformations moving to a false region. The constraints were then removed and the structure was subjected to 500 cycles minimization. MMFF94 force field<sup>16</sup> and partial atomic charges were used. Powell's<sup>17</sup> conjugate gradient method was used for minimization. The minimum energy difference of 0.05 KCal/mol was set as a convergence criterion. The most important input and most sensitive variable in CoMFA is the alignment, that is, molecular conformation and orientation. Molecule **23** was taken as the template and rest of the molecules were aligned to it using database alignment method in the Sybyl. The common substructure used for the alignment is shown in Scheme 2. The aligned molecules are shown in Figure 1.

#### CoMFA interaction energy calculation

The steric and electrostatic CoMFA<sup>18</sup> fields were calculated at each lattice intersection of a regularly spaced grid of 2.0 Å in all three dimensions within defined region. The van der Waals potential and coulombic terms representing the steric and electrostatic fields were calculated using standard Tripos force fields. A distance dependent dielectric constant of 1.00 was used. An sp<sup>3</sup> carbon atom with +1.00 charge was used as a probe

atom. The steric and electrostatic fields were truncated at +30.00 KCal/mol, and the electrostatic fields were ignored at the lattice points with maximal steric interactions.

#### Partial least square (PLS) analysis

PLS method was used to linearly correlate the CoMFA fields to the inhibitory activity values. The cross-validation<sup>19,20</sup> analysis was performed using leave-one-out (LOO) method in which one compound is removed from the dataset and its activity is predicted using the model derived from the rest of the dataset. The cross-validated  $r^2$  that resulted in optimum number of components and lowest standard error of prediction were considered for the further analysis. Equal weights were assigned to steric and electrostatic fields using COMFA\_STD scaling option. To speed up the analysis and reduce noise, a minimum filter value  $\sigma$  of 2.00 KCal/mol was used. Final analysis was performed to calculate conventional  $r^2$  using the optimum number of components. To further assess the robustness and statistical confidence of the derived models, bootstrapping analysis for 100 runs was performed.<sup>21</sup> All the cross-validated results were analyzed considering the fact that a value of  $r_{cv}^2$  above 0.3 indicates that probability of chance correlation is less than 5%.<sup>22</sup>

#### Predictive correlation coefficient ( $r_{pred}^2$ )

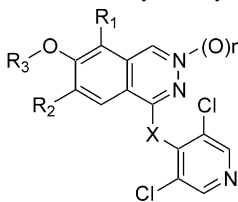
The predictive ability of each 3D-QSAR model was determined from a set of seven compounds that were not included in the training set. These molecules were aligned, and their activities were predicted. The predictive correlation coefficient ( $r_{pred}^2$ ), based on molecules of test set, is defined as

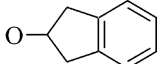
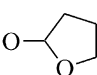
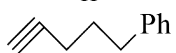
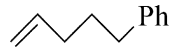
$$r_{pred}^2 = (\text{SD-PRESS})/\text{SD}$$

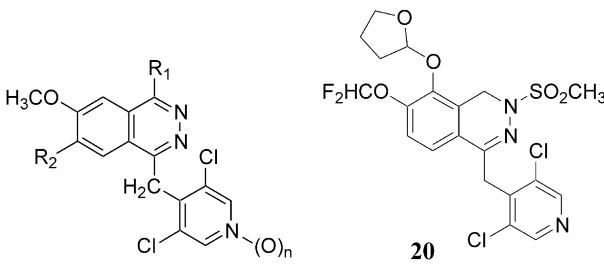
where SD is the sum of the squared deviations between the biological activities of the test set and mean activities of the training set molecules and PRESS is the sum of squared deviation between predicted and actual activity values for every molecule in test set.

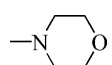
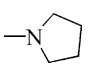
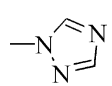
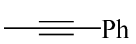
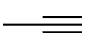
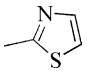
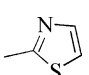
### Results and Discussion

The initial study of the 3D-QSAR analysis of phthalazines class of PDE IV inhibitors using CoMFA was carried out using Series 1 and 2. The in vitro PDE IV inhibition data using human neutrophil PDE IV were reported for these two series of phthalazine derivatives by the same research group.<sup>11a–c</sup> Since, the biological data was reported for the PDE IV target using the same source, human neutrophil PDE IV, and with quite a diverse substituents on the phthalazine ring, we combined Series 1 and 2 for CoMFA study. The total 21 molecules from Series 1 and 2 were considered for the analysis. The molecules **5** (phthalazine derivative) and **20** (dihydrophthalazine derivative) were dropped out of the analysis, as these two molecules contain a chiral center and the stereochemistry was not specified. Both

**Table 1.** Dataset used in the CoMFA analysis and their PDE IV inhibitory activity  
Series 1<sup>11a</sup>


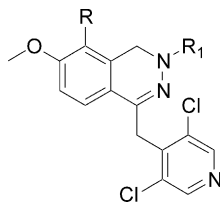
Molecule	X	R <sub>1</sub>	R <sub>2</sub>	R <sub>3</sub>	n	IC <sub>50</sub> (nM)
1	CH <sub>2</sub>	O–cC <sub>5</sub> H <sub>9</sub>	H	CH <sub>3</sub>	0	53
2	NH	O–cC <sub>5</sub> H <sub>9</sub>	H	CH <sub>3</sub>	0	59
3	CH <sub>2</sub>		H	CH <sub>3</sub>	0	30
4	CH <sub>2</sub>	O(CH <sub>2</sub> ) <sub>5</sub> Ph	H	CH <sub>3</sub>	0	57
5	CH <sub>2</sub>		H	CH <sub>3</sub>	0	153
6	CH <sub>2</sub>	O–cC <sub>5</sub> H <sub>9</sub>	H	CHF <sub>2</sub>	0	39
7	CH <sub>2</sub>	O–cC <sub>5</sub> H <sub>9</sub>	H	CH <sub>3</sub>	1	42
8	CH <sub>2</sub>	H	O–cC <sub>5</sub> H <sub>9</sub>	CH <sub>3</sub>	0	186
9	CH <sub>2</sub>		H	CH <sub>3</sub>	0	10
10	CH <sub>2</sub>		H	CH <sub>3</sub>	0	19
11	CH <sub>2</sub>	(CH <sub>2</sub> ) <sub>5</sub> Ph	H	CH <sub>3</sub>	0	30

Series 2<sup>11b,11c</sup>


Molecule	n	R <sub>1</sub>	R <sub>2</sub>	IC <sub>50</sub> (nM)
12	0		H	132
13	0		H	38
14	0		H	241
15	0	OPh	H	132
16	0	Ph	H	37
17	0		H	48
18	0		H	93
19	0		H	14
21	0	CH <sub>3</sub>	O–cC <sub>5</sub> H <sub>9</sub>	146
22	0	C <sub>2</sub> H <sub>5</sub>	O–cC <sub>5</sub> H <sub>9</sub>	75
23	1		H	4

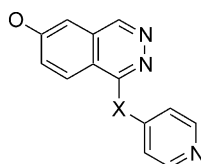
(continued)

Table 1 (continued)

Series 3<sup>11d</sup>

Molecule	R	R <sub>1</sub>	IC <sub>50</sub> (nM)
24	O- <i>c</i> C <sub>5</sub> H <sub>9</sub>	COCH <sub>3</sub>	30
25	O- <i>c</i> C <sub>5</sub> H <sub>9</sub>	SO <sub>2</sub> CH <sub>3</sub>	2
26	H	COCH <sub>3</sub>	51
27	H	COCH <sub>2</sub> CH <sub>3</sub>	28
28	H	COCH(CH <sub>3</sub> ) <sub>2</sub>	25
29	H	COPh	30
30	H	COCH <sub>2</sub> Ph	12
31	H	SO <sub>2</sub> CH <sub>3</sub>	21
32	H	COCO <sub>2</sub> CH <sub>2</sub> CH <sub>3</sub>	113
33	H	CO <sub>2</sub> CH <sub>3</sub>	72
34	H	CONH <sub>2</sub>	36
35	H	CONHCH <sub>3</sub>	131
36	H	CONHOH	85

the enantiomers of **5** and **20** were predicted later using the CoMFA model. A CoMFA model containing 17 molecules in the training set and four molecules in test set (**8**, **12**, **16** and **22**) was constructed from Series 1 and 2. The test set was selected randomly from the dataset. The statistics of the model were, the LOO cross-validation correlation coefficient  $r_{cv}^2$  0.546, optimum number of components 5, conventional correlation coefficient  $r^2$  0.999, standard error of estimate 0.018 and predictive correlation coefficient  $r_{pred}^2$  of 0.75. The model was statistically significant and predictive enough. The test set prediction was also found to be good as indicated by the predictive correlation coefficient. The stereoisomers of **5** and **20** were predicted using this CoMFA model. The activities of both the isomers of **5** as well as **20** were predicted to be almost same with residual of 0.34 for **5** and residual of 0.55 for **20**, respectively. The CoMFA model with 17 molecules in the training set may not cover all space and functional groups, there was a need to incorporate some more molecules in the model and improve the robustness of the model. The molecules, which can be incorporated to improve the predictivity and robustness of the existing model, should have the in vitro biological data using the same source of PDE IV (human neutrophil PDE IV as in Series 1 and 2) and preferably from the same research lab. Recently, we came across the data on some of the dihydropthalazine<sup>11d</sup> derivatives have been reported as PDE IV inhibitors by the same research group<sup>11a–c</sup> using the human neutrophil PDE IV. The Series 3<sup>11d</sup> comprises of 13 dihydropthalazine derivatives with the inhibitory data of PDE IV. All the three series of



Scheme 2.

molecules, total 34, were compiled together and a CoMFA model was reconstructed. For building the final CoMFA model, the test set was selected randomly.

The CoMFA model with 27 molecules in training set and seven molecules in test set resulted in a cross-validated correlation coefficient  $r_{cv}^2$  of 0.507 with minimum standard error and optimum number of components. This analysis was used for final non-cross validated run, giving a conventional correlation coefficient  $r^2$  of 0.980 with a low standard error of estimate. The contributions of steric and electrostatic CoMFA fields were obtained in a ratio of 0.6:0.4. To test the predictive ability of the resulting model, a test set of seven molecules excluded from the model creation work was used. The predictive correlation coefficient  $r_{pred}^2$  of 0.59 indicates the good

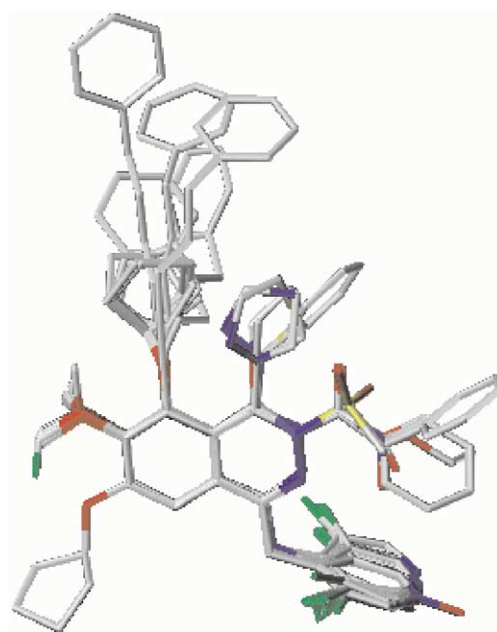


Figure 1. Alignment of the training set molecules.

external predictivity of the model. A high  $r^2$  value of 0.991 during 100 runs of bootstrapped analysis further supports the statistical validity of the model. The results of Partial Least Square (PLS) analysis are shown in the Table 2. The actual, predicted values by the model and residuals for training set and test set are given in Tables 3 and 4, respectively. A plot of predicted versus actual inhibitory activity of training set molecules is shown in the Figure 2. The QSAR produced by CoMFA, with its hundreds or thousands of terms, was represented as a 3D ‘coefficient contour’. Colored contours in the map represent those areas in 3D space where changes in the

steric and electrostatic field values of those compounds correlate strongly with concomitant change in the biological activities. The final CoMFA gives contour plots of steric and electrostatic interactions. The steric interactions are represented by green- and yellow-colored contours while electrostatic interactions are represented by red- and blue-colored contours. The bulky substituents are favored in green regions and disfavored in yellow regions. The increasing positive charge is favored in blue regions while increasing negative charge is favored in red regions. The CoMFA steric and electrostatic fields for the analysis of the final CoMFA model are presented as contour plots in Figures 3 and 4, respectively. To aid in the visualization, the template molecule **23** is also displayed in the maps.

Several electrostatic red contours are seen near the thiazole ring of the template molecules in the final CoMFA model contour plots. There are three red contours near the ring nitrogen of the thiazole attached at C4 of the phthalazine nucleus. There are two small red contours away from the thiazole ring of the template molecule. In these regions, the substituents with high electronegativity or electron density may improve the affinity for the catalytic center of the PDE IV enzyme. The electrostatic blue contours are seen above and below the plane of dichloropyridine ring of the template molecule. There is a big contour near methyl of C6-methoxy group of template. A blue contour is also seen near sulphur and C5 of the thiazole ring of the template molecule. These are the regions where the substituents with lower electron density are favored for the PDE IV

**Table 2.** Summary of final CoMFA model statistics

Parameter	CoMFA
$r_{cv}^2$	0.507
SDEP	0.379
$N$	6
$r^2$	0.980
SEE	0.077
F-test value	161.118
Prob. of $r^2 = 0$	0.00
PRESS	0.39
SD	0.96
$r_{pred}^2$	0.59
$r_{bs}^2$	0.991
Contributions	
Steric field	0.596
Electrostatic field	0.404

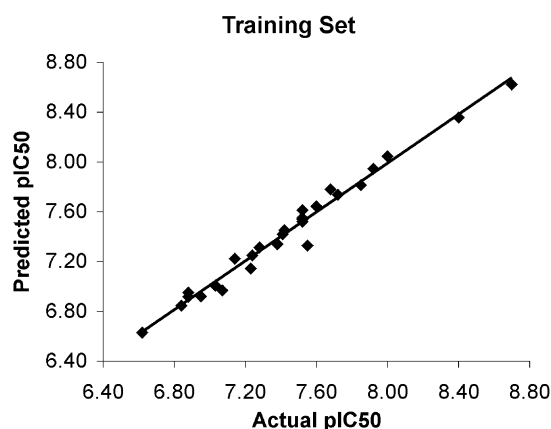
[ $r_{cv}^2$ , cross-validated correlation coefficient;  $N$ , no. of components; SDEP, standard error of prediction;  $r^2$ , conventional correlation coefficient; SEE, standard error of estimate; PRESS, predicted residual sum of squares of test set molecules; SD, standard deviation for the test set molecules;  $r_{pred}^2$ , predictive correlation coefficient;  $r_{bs}^2$ , correlation coefficient after 100 runs of bootstrapping analysis].

**Table 3.** Actual and predicted inhibitory activities (pIC<sub>50</sub>) and residuals of the training set molecules for final CoMFA model

Molecule	Actual pIC <sub>50</sub>	Predicted pIC <sub>50</sub>	Residual
1	7.28	7.32	−0.04
2	7.23	7.15	0.09
3	7.52	7.54	−0.02
4	7.24	7.25	−0.01
6	7.41	7.42	−0.01
7	7.38	7.34	0.04
9	8.00	8.05	−0.04
10	7.72	7.74	−0.02
11	7.52	7.52	0.00
13	7.42	7.45	−0.03
14	6.62	6.63	−0.01
15	6.88	6.92	−0.04
18	7.03	7.01	0.02
19	7.85	7.81	0.04
21	6.84	6.85	0.00
23	8.40	8.36	0.04
24	7.52	7.61	−0.09
25	8.70	8.62	0.08
27	7.55	7.33	0.22
28	7.60	7.65	−0.04
29	7.52	7.55	−0.03
30	7.92	7.95	−0.03
31	7.68	7.78	−0.10
32	6.95	6.92	0.03
33	7.14	7.22	−0.08
35	6.88	6.95	−0.07
36	7.07	6.97	0.10

**Table 4.** Actual and predicted inhibitory activities (pIC<sub>50</sub>) and residues of the test set molecules for final CoMFA model

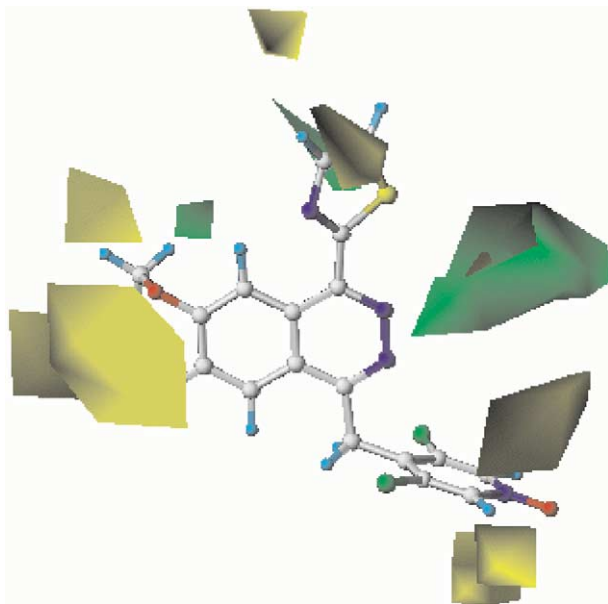
Molecule	Actual pIC <sub>50</sub>	Predicted pIC <sub>50</sub>	Residues
8	6.73	6.71	0.02
12	6.88	7.00	−0.12
16	7.43	7.34	0.09
17	7.32	7.19	0.13
22	7.12	6.85	0.27
26	7.29	7.00	0.29
34	7.44	7.00	0.44



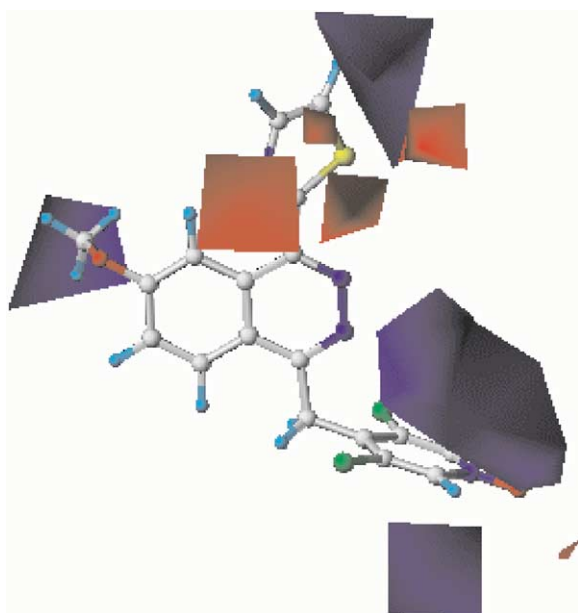
**Figure 2.** Plot of predicted versus actual pIC<sub>50</sub> of CoMFA training set molecules.



inhibitory activity. The molecules **25** and **31** contain N3-sulphonamide oxygen near the red contours favoring the electronegative substituents in these regions and hence they exhibit good inhibitory activity. **25** has an additional C5-cyclopentyloxy group where the oxygen is near a big red contour, therefore **25** is more potent than **31**. The molecules **24**, **27**, **28**, **29** and **30** also exhibit good inhibitory activity as N3-amide oxygen is near electron density favoring red contours. The molecules **24** and **25** are same except the difference at N3, where **24** contains a carbonyl while **25** contains a sulphonyl group, the additional oxygen of the sulphonyl increases



**Figure 3.** CoMFA STDEV\*COEFF contour maps for steric field. The molecule **23** is displayed in the background.



**Figure 4.** CoMFA STDEV\*COEFF contour maps for electrostatic field. The molecule **23** is displayed in the background.

the electron density in that regions near the electrostatic red contours, hence **25** exhibit better inhibitory activity than **24**. The orientation of the electronegative groups in the regions near N3 of the phthalazine ring also plays an important role in determining the activity as seen from the activities of **33** and **26**, where **26** contains acetyl group at N3 while **33** contains methyl ester at N3. The additional oxygen of ester at N3 in **33** is oriented towards electropositive blue contours; therefore, **33** exhibits slight lower inhibitory activity than **26**. In the molecules **34** and **35** the carbonyl at N3 is near red contours but additional ester attached to carbonyl in **34** and additional nitrogen attached to carbonyl in **35** are oriented towards the electropositive blue contours, hence these molecules also exhibit low inhibitory activity. The molecule **13** contains a pyrrolidine substituent at C4 where the N of pyrrolidine is close to electronegative group favoring red contours and hence **13** exhibits good inhibitory potency. The molecule **14**, similar to **13**, contains a triazole at C4 of phthalazine where the two nitrogens of the triazole ring are close to red contours but the third nitrogen is close to electronegative group disfavoring blue contours, hence it exhibits very low inhibitory activity. The molecule **2** is an isostere of **1**, the linker –NH– in **2** slightly disturbs the orientation of dichloropyridine and do not affect the molecular recognition by the active site as reflected in their almost same biological activity. The molecule **15** contains a phenoxy group at C4 of the phthalazine ring where the electron density reach phenyl group is enclosed in a blue contour where low electron density is favored, therefore it exhibits low activity.

The steric green contours of the final CoMFA model show a green contour forming a small cavity near N3 of the phthalazine ring indicating the preference for bulkier substituents in that region. There is seen a small green contour near thiazole ring of the template molecule and a green contour near C6 methoxy group. The molecules with N3 substituents and containing proper functional groups orient the N3 substituents toward the sterically favorable green region and exhibit good activity like molecules **25**, **28**, **29**, **30**, and **31**. The molecule **30** is more potent than **29**, where **30** contains a phenacyl group at N3 while **29** contain a benzoyl group at N3, as additional methylene group in **30** orients the terminal phenyl in the green contour cavity where bulky substituent is favored. The nature of the functional groups present at N3 determines the orientation of the substituent at N3. The additional ester group at N3 in the molecule **32** orients terminal ethyl group away from the green contour region and it exhibits less activity than **27** where the carbonyl at N3 orients terminal ethyl in the green contour cavity. There are several steric yellow contours seen where the bulkier substituents may decrease the PDE IV affinity of the inhibitors. There are three yellow contours seen above and below the plane of the dichloropyridine ring of the inhibitors. There is a yellow contour near the methoxy group at C6 and two more yellow contours near the C7 of the phthalazine nucleus. Near the thiazole ring of the template molecule, two yellow contours are observed. The orientation of the methoxy group at C6 is important for the molecular

recognition by PDE IV active site. Depending upon the presence or absence of the substituents at C5 and C7, and the nature of the substituents when present, the methoxy group at C6 orients differently. The molecule **21** exhibits a cyclopentyloxy substituent at C7, which clashes with the sterically unfavorable yellow contours in that region and also due to steric interactions the methoxy at C6 orients towards the yellow contour and this molecule exhibit lower inhibitory activity. When long chain substituents are present on the phthalazine ring, their conformational flexibility affects the biological activity. Comparing the molecule **9**, **10** and **11**; the long chain substituent at C5 changes from acetylinic in **9** to ethylenic in **10** to ethylene in **11**, the conformational flexibility increases and the biological activity decreases as possibility of steric clash in sterically unfavorable region increases.

The molecules **5** and **20**, which were excluded from the analysis due to their unknown stereochemistry, were also predicted using the final CoMFA model. Both the isomers of **5** as well as **20** were predicted to be of almost same biological activity, with residual of 0.25 for **5** and residual of 0.08 for **20** respectively, by the final model as by the previous model from Series 1 and 2. This shows that the stereochemistry at tetrahydrofuran substituent at C5 of phthalazine ring may not be crucial for the biological activity and hence for PDE IV active site recognition by **5** and **20**. These two molecules were predicted better by the final CoMFA model than the previous model.

The final CoMFA model with statistically significant parameters correlates the variation in the biological activities of the phthalazine and dihydrophthalazine class of PDE IV inhibitors with the changes in the electrostatic and steric fields around the molecules.

### Conclusion

The CoMFA model described herein shows good internal ( $r^2$ ) and external ( $r^2_{\text{pred}}$ ) consistency, which indicates the statistically valid model with good correlative and predictive power. It provides the information on the effect of the electrostatic and steric fields around the aligned molecules on their biological activities. This study offers structural insight to aid in the development of novel and more potent PDE IV inhibitors.

### References and Notes

- Perry, M. J.; Higgs, G. A. *Curr. Opin. Chem. Biol.* **1998**, *2*, 472.
- Soderling, S. H.; Beavo, J. A. *Curr. Opin. Cell. Biol.* **2000**, *12*, 174.
- Domenico, S. *Curr. Opin. Invest. Drugs* **2000**, *1*, 204.
- Giembycz, M. A. *Drugs* **2000**, *59*, 193.
- Wang, P.; Myers, J. G.; Wu, P.; Cheewatrakoolpong, B.; Egan, R. W.; Billah, M. M. *Biochem. Biophys. Res. Comm.* **1997**, *234*, 320.
- Muller, T.; Engels, P.; Fozard, J. R. *Trends Pharmacol. Sci.* **1996**, *17*, 294.
- Marivet, M.; Bourguignon, J.; Lugnier, C.; Mann, A.; Stoclet, J.; Wermuth, C. J. *Med. Chem.* **1989**, *32*, 1450.
- Piaz, V. D.; Giavannoni, M. P. *Eur. J. Med. Chem.* **2000**, *35*, 463.
- Asthan, M. J.; Cook, D. C.; Fenton, G.; Karlsson, J.; Paley, M. N.; Raesburn, D.; Ratcliffe, A. J.; Souness, J. E.; Thurairatnam, M. N.; Vicker, N. J. *Med. Chem.* **1994**, *37*, 1696.
- Burnouf, C.; Pruniaux, M. *Curr. Pharm. Des.* **2002**, *8*, 1255.
- (a) Neapolitano, M.; Norcini, G.; Pellacini, F.; Marchini, F.; Morazzoni, G.; Ferlenga, P.; Pradella, L. *Bioorg. Med. Chem. Lett.* **2000**, *10*, 2235. (b) Neapolitano, M.; Norcini, G.; Pellacini, F.; Marchini, F.; Morazzoni, G.; Ferlenga, P.; Pradella, L. *Bioorg. Med. Chem. Lett.* **2001**, *11*, 33. (c) Neapolitano, M.; Norcini, G.; Pellacini, F.; Marchini, F.; Morazzoni, G.; Ferlenga, P.; Pradella, L. WO/99 32456, 1999. (d) Neapolitano, M.; Norcini, G.; Pellacini, F.; Marchini, F.; Morazzoni, G.; Ferlenga, P.; Fattori, R.; Pradella, L. *Bioorg. Med. Chem. Lett.* **2002**, *12*, 5.
- Cramer, R. D., III; Patterson, D. E.; Bunce, J. D. *J. Am. Chem. Soc.* **1988**, *110*, 5959.
- Desiraju, G. R.; Gopalakrishnan, B.; Jetty, R. K.; Nagaraju, A.; Raveendra, D.; Sarma, J. A.; Sobhia, M. E.; Thilagavathi, R. *J. Med. Chem.* **2002**, *45*, 4847.
- Desiraju, G. R.; Sarma, J. A.; Raveendra, D.; Gopalakrishnan, B.; Thilagavathi, R.; Sobhia, M. E.; Subramanya, H. S. *J. Phys. Org. Chem.* **2001**, *14*, 481.
- SYBYL 6.6; Tripos Associates Inc.: 1699 S Hanley Rd., St. Louis, MO 63144, USA.
- Halgren, T. *J. Am. Chem. Soc.* **1990**, *112*, 4710.
- Powell, M. J. D. *Mathemat. Prog.* **1977**, *12*, 241.
- Clark, M.; Cramer, R. D., III; Jones, D. M.; Patterson, D. E.; Simeroth, P. E. *Tetrahedron Comput. Methodol.* **1990**, *3*, 47.
- Cramer, R. D., III; Bunce, J. D.; Patterson, D. E. *Quant. Struct. Act. Relat.* **1988**, *7*, 18.
- Podlogar, B. L.; Ferguson, D. M. *Drug. Des. Discov.* **2000**, *17*, 4.
- Murthi, V. S.; Kulkarni, V. M. *Bioorg. Med. Chem.* **2002**, *10*, 2267.
- Clark, M.; Cramer, R. D., III *Quant. Struct. Act. Relat.* **1993**, *12*, 137.